

# NUCLEOSYNTHESIS IN GAMMA-RAY BURST ACCRETION DISKS

Jason Pruet<sup>1</sup>, S. E. Woosley<sup>2</sup>, and R. D. Hoffman<sup>1</sup>

<sup>1</sup>*N-Division, Lawrence Livermore National Laboratory, Livermore CA 94550* <sup>2</sup>*Department of Astronomy and Astrophysics, University of California, Santa Cruz, CA 95064*

## ABSTRACT

We follow the nuclear reactions that occur in the accretion disks of stellar mass black holes that are accreting at a very high rate,  $0.01$  to  $1 M_{\odot} \text{ sec}^{-1}$ , as is realized in many current models for gamma-ray bursts (GRBs). The degree of neutronization in the disk is a sensitive function of the accretion rate, black hole mass, Kerr parameter, and disk viscosity. For high accretion rates and low viscosity, material arriving at the black hole will consist predominantly of neutrons. This degree of neutronization will have important implications for the dynamics of the GRB producing jet and perhaps for the synthesis of the  $r$ -process. For lower accretion rates and high viscosity, as might be appropriate for the outer disk in the collapsar model, neutron-proton equality persists allowing the possible synthesis of  $^{56}\text{Ni}$  in the disk wind.  $^{56}\text{Ni}$  must be present to make any optically bright Type I supernova, and in particular those associated with GRBs.

*Subject headings:* gamma rays: bursts—nucleosynthesis—accretion disks

## 1. INTRODUCTION

Growing evidence connects GRBs to the the birth of hyper-accreting black holes (Fryer, Woosley, & Hartmann 1999), that is stellar mass black holes accreting matter from a disk at rates from  $\sim 0.01$  to  $10 M_{\odot} \text{ sec}^{-1}$ . Such models include the collapsar (Woosley 1993; MacFadyen & Woosley 1999), merging neutron stars and black holes (Eichler et al. 1989; Janka et al. 1999, 2001), supranovae (Vietri & Stella 1998, 1999), merging helium cores and black holes (Zhang & Fryer 2001), and merging white dwarfs and black holes (Fryer et al. 1999). For such high accretion rates the disk is optically thick, except to neutrinos, and very hot, consisting in its inner regions of a (viscous) mixture of neutrons and protons. At its inner boundary the disk connects to the black hole. Whatever processes accelerate the

putative GRB-producing jet might therefore be expected to act upon some mixture of disk material and other background medium (e.g., the collapsing star in the collapsar model). Farther out, material will be lost from the disk in a vigorous wind (MacFadyen & Woosley 1999; Narayan, Piran, & Kumar 2002). In fact, Narayan et al. suggest that *most* of the disk will be lost to a wind except for those models and in those regions where neutrino losses dominate the energy budget.

It is thus of some consequence to know the composition of such disks. In the least case, the nucleosynthesis may be novel and could account for rare species in nature, such as the *r*-process. At most, the presence of free neutrons may affect the dynamics of the GRB jet (Derishev, Kocharovsky, & Kocharovsky 1999; Fuller, Pruet, & Abazajian 2000), the GRB neutrino signature (Bahcall & Mészáros 2000), light curve (Pruet & Dalal 2002), and afterglow (e.g. via a “pre-acceleration” mechanism similar to the one discussed by Beloborodov 2002). It is also of some consequence to know whether the disk wind consists of radioactive  $^{56}\text{Ni}$ , as is necessary if a visible supernova is to accompany the GRB. If the electron mole number,  $Y_e = \Sigma(Z_i X_i / A_i)$ , is less than 0.485, the iron group will be dominated by  $^{54,56}\text{Fe}$  and other more neutron-rich species (Hartmann, Woosley, & El Eid 1985) which will be incapable of illuminating the supernova. Since the jet itself is inefficient at heating sufficient matter to temperatures required for nuclear statistical equilibrium ( $T \gtrsim 5 \times 10^9$  K), supernovae seen in conjunction with GRBs (Galama et al. 1998; Bloom et al. 2002, for example) would be difficult to understand.

We have thus undertaken a survey of the nucleosynthesis that happens in the disks of rapidly accreting black holes. The work is greatly facilitated by the existence of numerical and semi-analytic solutions that yield the temperature-density structure and drift velocity (Popham, Woosley, & Fryer 1999). These solutions have been verified in the case of the collapsar model by direct numerical simulation (MacFadyen & Woosley 1999).

## 2. COMPUTATIONAL APPROACH

For a disk that is optically thin to neutrinos the neutron to proton ratio,  $n/p$ , is determined by the competition between electron and positron capture on nuclei and free nucleons. Since the baryon number per co-moving volume is conserved, it is convenient to work with the electron fraction  $Y_e$  defined by

$$Y_e = \Sigma Z_i (X_i / A_i) \quad (1)$$

where  $Z_i$ ,  $X_i$ , and  $A_i$  are the proton number, mass fraction, and atomic mass number (integer) of the species  $i$ . We shall refer to compositions with  $Y_e < 0.5$  as “neutron-rich”.

If we neglect lepton capture on bound nuclei and approximate the disk material as consisting of a mixture of free nucleons and  $\alpha$ -particles, the evolution of  $Y_e$  with radius is given by

$$\mathbf{u} \cdot (\nabla Y_e) = V(r) \sqrt{\frac{1 - 2GM/rc^2}{1 - (V(r)/c)^2}} \frac{dY_e}{dr} = -\lambda_{e^-p} \left( Y_e - \frac{1 - X_n}{2} \right) + \lambda_{e^+n} \left( 1 - Y_e - \frac{1 - X_n}{2} \right). \quad (2)$$

Here  $X_n$  is the mass fraction of free nucleons,  $\mathbf{u}$  is the 4-velocity of the flow,  $M$  represents the black hole mass, and  $V(r)$  is the radial drift velocity as measured in an inertial frame co-rotating with the disk. In the middle term in Eq. 2 we have assumed steady state conditions as well as cylindrical symmetry, and we have adopted the relatively simple Schwarzschild metric relevant for most of our calculations. Generally, relativistic effects do not make a big difference in our calculations of the electron fraction, though they are important for determining the structure of the disk.

In Eq. 2  $\lambda_{e^-p}$  and  $\lambda_{e^+n}$  are the rates for the processes

$$e^- + p \rightarrow n + \nu_e \quad (3)$$

$$e^+ + n \rightarrow p + \bar{\nu}_e. \quad (4)$$

These rates are given by

$$\lambda_{e^-p} = K \int_{\frac{\delta m}{m_e}}^{\infty} w^2 \left( w - \frac{\delta m}{m_e} \right)^2 G_-(1, w) S_-(T, U_F) dw \quad (5)$$

$$\lambda_{e^+n} = K \int_0^{\infty} w^2 \left( w + \frac{\delta m}{m_e} \right)^2 G_+(1, w) S_+(T, U_F) dw. \quad (6)$$

Here  $K \approx 6.414 \cdot 10^{-4} \text{s}^{-1}$  determines the free neutron lifetime,  $\delta m \approx 1.293 \text{ MeV}$  is the neutron proton mass difference, and  $m_e$  is the electron mass. The functions  $S_-$  and  $S_+$  are the electron and positron distribution functions, while the  $G_{\pm}$  are the Coulomb wave correction factors discussed in Fuller, Fowler, & Newman (1982).

The electron Fermi energy  $U_F$  is found by inverting the expression for the net electron number density,

$$n_e^- - n_e^+ = \rho Y_e N_A = \frac{1}{\pi^2} \left( \frac{m_e c}{\hbar} \right)^3 \int_0^{\infty} p^2 (S_-(T, U_F) - S_+(T, U_F)) dp \quad (7)$$

with  $p = \sqrt{w^2 - 1}$ .

We solve for the evolution of  $Y_e$  by integrating eq. 2 for the results presented in Popham, Woosley, & Fryer (1999). Those authors assumed  $Y_e = 1/2$ . Because we will show that in

some cases  $Y_e \ll 1/2$ , and consequently that the electron Fermi energy and degeneracy pressure are substantially smaller than for  $Y_e = 1/2$ , our results are not entirely self consistent, but should suffice given the very approximate nature of a one-dimensional calculation.

### 3. RESULTS

#### 3.1. Scaling with Disk Viscosity and Accretion Rate

We present results for several different disk models. The parameters describing these models, as well as the electron fraction near the event horizon at  $r \approx 10^6 \text{cm}$ , are given in Table 1. In all cases we assume  $Y_e = 1/2$  at large radii. For simplicity we have adopted a constant black hole mass of  $3 M_\odot$  though the scaling relations for mass are obvious in Popham et al. All else being equal, a larger mass will give less electron capture.

Table 1 shows a clear trend with disk viscosity and accretion rate: electron capture in the inner disk becomes more pronounced with decreasing viscosity and increasing mass accretion rate. This arises because low viscosity flows inefficiently advect angular momentum outwards and are, for a given mass accretion rate, denser than high viscosity flows. Dense flows are electron degenerate, so that pair  $e^\pm$  creation is suppressed and electron capture dominates over positron capture. Similarly a larger accretion rate also implies a denser disk - for a given value of  $\alpha$  - and more capture.

Before discussing in some detail the evolution of  $Y_e$  in our calculations we note that the influence of black hole spin on the composition is also important. This is because the angular momentum imparted to the black hole via the accreting matter will typically drive the Kerr parameter high. For example, a Kerr parameter of  $a \sim 0.9$  is typical for collapsars. A larger Kerr parameter allows the disk to move to smaller radii before entering the event horizon, so that more electron capture and a smaller  $Y_e$  will result. This is demonstrated by model G, which corresponds to a black hole with  $a = 0.95$ . In this model  $n/p$  near the event horizon is about ten times larger than  $n/p$  for the same model except with  $a = 0$  (model B). The influence of the black hole spin on  $Y_e$  is limited to regions quite near the event horizon. For  $r > 10^{6.5} \text{cm}$ ,  $Y_e$  in model B is essentially the same as in model G. These considerations imply that as far as the composition is concerned, the main difference between flows around zero angular momentum holes and those around large angular momentum holes will be that the jet in the large angular momentum case will likely be more neutron rich. The composition in the bulk of the wind coming from the disk, however, will likely be similar in the two cases.

In Fig. 1 we show the evolution of  $Y_e$  with radius for an accretion disk with  $\alpha = 0.1$  and a relatively low mass accretion rate (at least for standard collapsar models),  $\dot{M} =$

$0.01 M_{\odot} \text{ sec}^{-1}$ . This flow is not dense enough to drive the electrons degenerate. Consequently  $Y_e$  is governed by thermal  $e^{\pm}$  capture. In this case the only asymmetry is the neutron-proton mass difference and  $Y_e$  actually increases slightly owing to the threshold for the rate in Eq. 3, becoming greater than 0.5. The free nucleon mass fraction appearing in Fig. 1 is calculated from the simple estimate provided in Qian & Woosley (1996). Lepton capture on heavy nuclei is negligible for this disk.

Results for a hotter and denser flow,  $\dot{M} = 0.1 M_{\odot} \text{ sec}^{-1}$ ,  $\alpha = 0.1$ , are shown in Fig. 5. The material at radii  $r \lesssim 10^{7.5} \text{ cm}$  is mildly degenerate and the electron fraction is driven to  $Y_e \approx 0.44$ . The quantity  $\lambda_{e-p}(r/V)$  is the product of the electron capture rate and a rough measure of the dynamic timescale, or time left before the infalling material crosses the event horizon. Because  $Y_e$  can not come to equilibrium unless  $\lambda_{e-p}(r/V) \approx 1$ ,  $Y_e$  is not in equilibrium in this flow. Also, because  $\lambda_{e-p}(r/V) \ll 1$  when bound nuclei are present, weak processes on heavy nuclei are not important even in the extreme limit where the bound nucleons behave as free nucleons with respect to electron capture.

Figures 3 and 4 show the influence of viscosity on the composition of the flow. For  $\alpha = 0.03$  electron capture becomes important at  $r \approx 10^{7.6} \text{ cm}$  and  $Y_e$  is in close equilibrium with  $e^{\pm}$  capture until  $r \approx 10^{6.5} \text{ cm}$ . There is at most  $\sim 1/10$  of an electron capture per bound nucleus in the disk. For  $\alpha = 0.01$  the inflowing material becomes degenerate and neutron rich early on. Most of the free protons are locked into  $\alpha$ -particles until the  $\alpha$ -particles dissociate. Positron capture on the excess free neutrons results in a brief *increase* in  $Y_e$ , as seen in the bump at  $r \approx 10^{7.3} \text{ cm}$  in Fig. 2. The final  $n/p$  in this disk is very large,  $\sim 20$ .

The influence of the mass accretion rate on the composition is seen in Fig. 5, where we plot results for  $\dot{M} = 1 M_{\odot} \text{ sec}^{-1}$  and  $\alpha = 0.1$ . This disk is quite similar to the  $\dot{M} = 0.1 M_{\odot} \text{ sec}^{-1}$ ,  $\alpha = 0.3$  case. Indeed, this is just what is expected from the scaling relations in Popham, Woosley, & Fryer (1999). For  $\dot{M} \approx 1 M_{\odot} \text{ sec}^{-1}$  and larger, the assumption that the disk is optically thin to neutrinos begins to break down (MacFadyen & Woosley 1999; Di Matteo, Perna, & Narayan 2002). This influences both the structure of the disk, and, because neutrino capture becomes important, the evolution of  $Y_e$ . Because neutrino trapping likely influences the structure of the disk at the same level as the assumption that  $Y_e = 1/2$ , we do not calculate  $Y_e$  for disks calculated under the assumption of partial neutrino trapping (and  $Y_e = 1/2$ ).

### 3.2. Effects of Neutrino Capture

The effect of neutrino capture on the evolution of  $Y_e$  can be addressed in an approximate way. In particular, we are interested in the rate  $\lambda_{\nu_e n}$  for the process

$$\nu_e + n \rightarrow p + e^-. \quad (8)$$

The rate for  $\bar{\nu}_e$  capture is suppressed both because of the low proton number density and the absence of high energy positrons in the flow. The number of neutrinos captured per neutron is roughly  $\tau_{\nu_e, \text{cap}} n_{\nu_e} / n_n \approx Y_e \tau_{\nu_e, \text{cap}} n_{\nu_e} / n_p$ , where  $\tau_{\nu_e, \text{cap}}$  is the optical depth for the process in Eq. 8, and  $n_{\nu_e} / n_n$  ( $n_{\nu_e} / n_p$ ) is the number of electron neutrinos produced per neutron (proton) in the flow. The ratio  $R$  of the number of neutrino captures per neutron to the number of electron captures per proton is

$$R \approx \frac{\lambda_{\nu_e}}{\lambda_{e^- p}} = \tau_{\nu_e, \text{cap}} Y_e. \quad (9)$$

This equation implies that an optical depth of 1 to  $\nu_e$  capture is roughly equivalent to a doubling of  $\lambda_{e^+ n}$ . We note here that while the  $\nu_e$ 's produced in electron-capture reactions are not thermal, their average capture cross section is only approximately a factor of 2 higher than the average capture cross section calculated under the assumption of a thermal distribution for the electron neutrinos (at the electron Fermi energy and temperature) for conditions of interest in accretion disks.

It is difficult to quantitatively calculate the influence of neutrino capture on  $Y_e$  in a post-processing step. This is both because of the complexities of neutrino transport, as well as because of the feedback between  $Y_e$ , the electron capture rate, and the disk dynamics. However, the following simple considerations argue that neutrino capture is unlikely to have a dramatic influence on  $Y_e$ .

To discuss some specific cases, consider first the  $\dot{M} = 0.1 M_\odot \text{sec}^{-1}$ ,  $\alpha = 0.1$  disk. Di Matteo, Perna, & Narayan (2002) argue that neutrinos will have an absorptive optical depth of unity at  $r \approx 3 \cdot 10^6 \text{cm}$  for this disk. Because weak processes have essentially frozen out by this radius (see the  $\lambda_{e^- p}(r/V)$  curve in Fig. 2), neutrino capture will have a small influence on  $Y_e$ .

Denser flows trap neutrinos more efficiently but are still expected to remain neutron rich. For example, for the  $\dot{M} = 1 M_\odot \text{sec}^{-1}$ ,  $\alpha = 0.1$  disk, Di Matteo, Perna, & Narayan (2002) show that the neutrino absorptive optical depth will be greater than unity for  $r \lesssim 2 \cdot 10^7 \text{cm}$ . As weak processes are rapid compared to the dynamic timescale in this disk, the result will be an increase in  $Y_e$ . To estimate the magnitude of this increase we adopt the simple procedure of artificially increasing the positron capture rate,  $\lambda_{e^+ n} \rightarrow 5\lambda_{e^+ n}$ , which is likely

an overestimate of the protonization rate. The increase in  $\lambda_{e+n}$  results in an electron fraction of  $Y_e \approx 0.166$  near the event horizon. This is approximately 50% higher than the electron fraction calculated by neglecting the influence of  $\nu_e$  capture, though still quite neutron rich.

To summarize,  $Y_e$  in disks with high viscosity and modest accretion rates will not be affected by neutrino capture simply because neutrinos are not trapped or because weak processes are too slow. The electron fraction in disks with neutrino absorptive optical depths of a few will increase somewhat but will remain neutron rich owing to the sharp rise in  $\lambda_{e-p}$  with  $Y_e$ .

### 3.3. Transport to the Surface of the Disk

In order for a low electron fraction to have observable implications the electron fraction must not come to equilibrium at  $Y_e = 1/2$  as the material travels out of the plane of the disk. To estimate the evolution of the electron fraction in convective blobs moving out of the disk we parametrize the convective timescale by the turbulent convection speed (Narayan, Piran, & Kumar 2002)

$$v_{\text{turb}} \approx \alpha v_K = 6.3 \times 10^8 \alpha_{-1} r_7^{-1/2} \text{ cm s}^{-1} \quad (10)$$

where  $\alpha_{-1} = \alpha/0.1$  and  $r_7 = r/10^7 \text{ cm}$ . This implies a time to go one pressure scale height

$$\tau_{\text{conv}} \sim r/v_{\text{turb}} \sim 16 \alpha_{-1}^{-1} r_7^{1/2} \text{ ms}. \quad (11)$$

We also assume that the convective blob expands adiabatically. An estimate for the entropy per baryon in the disk is given by Qian & Woosley (1996):

$$s/k_b \approx 0.052 \frac{T_{\text{MeV}}^3}{\rho_{10}} + 7.4 + \ln \left( \frac{T_{\text{MeV}}^{3/2}}{\rho_{10}} \right). \quad (12)$$

Here  $T_{\text{MeV}}$  is the temperature in MeV and  $\rho_{10}$  is the density in units of  $10^{10} \text{ g cm}^{-3}$ . The first term on the right hand side of Eq. 12 is the contribution to the entropy from relativistic light particles ( $\gamma/e^\pm$ ), while the next two represent the contribution from free nucleons. Eq. 12 is not appropriate when electrons are degenerate. For degenerate electrons the contribution of thermal  $e^\pm$  pairs is small and the coefficient 0.052 should be closer to 0.02, representing just the entropy of the photons. However, changing the coefficient to 0.02 makes little difference for our purposes.

When relativistic particles dominate the entropy, the adiabat satisfies  $T^3 \propto \rho$ . When free nucleons dominate the entropy, the adiabat satisfies  $T^{3/2} \propto \rho$ . The evolution of the

electron fraction in a convective blob is crucially sensitive to the adiabat on which the blob travels.

To illustrate this, consider first a disk with  $\dot{M} = 0.01$ ,  $\alpha = 0.1$ . In Fig. 6 we show the evolution of the electron fraction in matter originating from two different points in this disk and for different assumptions about  $\tau_{\text{conv}}$ . The upper curves in Fig. 6 correspond to material originating from  $r = 10^{6.5}\text{cm}$  in the disk. At this point the entropy is relatively high,  $s/k_b \sim 23$  by the estimate in Eq. 12, and consequently the adiabat is closer to  $T^3 \propto \rho$  than to  $T^{3/2} \propto \rho$ . The temperature decreases quite slowly relative to the density, allowing for the formation of pairs which efficiently drive  $n/p$  to equality. For large  $\tau_{\text{conv}}$  this process occurs more efficiently than for small  $\tau_{\text{conv}}$ . The lower curves in Fig. 6 correspond to matter originating from  $r = 10^7\text{cm}$  in the disk. At this point the entropy is  $\approx 17$ , so the adiabat is near  $T^{3/2} \propto \rho$ . For low entropies, then, the temperature and density decrease at a comparable rate and pair formation is somewhat suppressed, keeping  $Y_e$  low.

For flows where the electron fraction is high enough to drive the inner disk neutron rich, the entropy is generally dominated by non-relativistic particles, and the adiabat again preserves a low  $Y_e$ . This is illustrated in Fig. 7 where we plot the evolution of electron fraction in an adiabatic convective bubble for two different disks characterized by a low  $Y_e$ . In this figure we only show the evolution of a fluid element from a single initial radius ( $10^7\text{cm}$ ) because the entropy in these disks is never dominated by relativistic particles when  $Y_e$  is low, so that the behavior shown in Fig. 7 is generic.

The above considerations outline the general features of how  $Y_e$  evolves in material as it travels from the center to the surface of the disk. In flows where  $Y_e$  is driven small, the degeneracy of the electrons implies that free nucleons dominate the entropy. A low  $Y_e$  then, will remain low. By contrast, in flows where  $Y_e$  is close to  $1/2$ , the adiabat can be close enough to  $T^3 \propto \rho$  for  $Y_e$  to be driven to  $1/2$ , and the neutron excess at the center of the disk is larger than the neutron excess in material finding its way out of the disk.

## 4. IMPLICATIONS

### 4.1. Radioactivity in the disk wind

The most obvious consequence of our calculations is that  $^{56}\text{Ni}$  will be absent from the winds of hyper-accreting black holes unless a) the accretion rate is low ( $\lesssim 0.1 M_\odot \text{sec}^{-1}$ ), and b) the disk viscosity is high,  $\alpha \gtrsim 0.1$ . Interestingly, modern views regarding  $\alpha$ -disks and GRB models favor values close to these.



Typical accretion rates in the collapsar model are  $0.05 - 0.1 M_{\odot} \text{ sec}^{-1}$  (MacFadyen & Woosley 1999, their figures 5 and 10). The neutron excess will be smaller in Type II collapsars powered by fall back rather than direct black hole formation (MacFadyen, Woosley, & Heger 2001). Considerable accretion into the hole and mass loss from the disk may continue, at a declining rate, even after the main GRB producing event ( $\sim 20$  s) is over (Zhang & Woosley 2002). It thus seems likely that the collapsar model will be able to provide the  $^{56}\text{Ni}$  necessary to make the supernovae that accompany GRBs (though only if  $\alpha \gtrsim 0.1$ ). This is also true of the slower accreting models like helium-star black hole mergers and black hole white dwarf mergers. However any wind from merging compact objects, or similar models like the supranova, will be neutron rich. Though perhaps of interest for nucleosynthesis, they will not produce  $^{56}\text{Ni}$ , at least during the black hole accretion epoch.

## 4.2. Neutron excess in GRB jets

For disks with high accretion rates, and certainly for merging neutron stars or black hole neutron star mergers, the matter near the event horizon will be very neutron rich. If this material pollutes the outgoing jet, the the GRB jet will itself, at least initially, contain free neutrons.

The dynamics of accelerating neutron-rich jets can differ dramatically from the dynamics of pure proton jets. Fuller, Pruet, & Abazajian (2000) showed that a high Lorentz factor fireball that is neutron rich can lead to two very distinct kinematic components, a slow neutron outflow and a fast proton outflow. This arises because the uncharged neutrons are weakly coupled to the radiation dominated plasma, and are accelerated principally via strong neutron-proton scatterings (Derishev, Kocharovsky, & Kocharovsky 1999). Strong scatterings freeze out when they become slow compared to the dynamic timescale and at this point the neutrons coast. If this decoupling occurs while the jet is still accelerating, then the coulomb-coupled protons go on to have a larger Lorentz factor than the neutrons.

Roughly, dynamic neutron decoupling is only expected for fast jets. Here the precise meaning of “fast” depends, among other things, the fireball source size. For relativistic flows originating from compact objects, the dynamic timescale characterizing the acceleration of the flow is about 1 ms and the final Lorentz factor must be greater than  $\sim 300$  in order for dynamic neutron decoupling to occur. For jets in the collapsar model, the timescale characterizing the acceleration is set by the surface of last interaction of the jet with the stellar envelope at  $\sim 10^{11}\text{cm}$ . In this case the final Lorentz factor of the jet has to be  $\gtrsim 3000$  for dynamic neutron decoupling to occur. Because this is an impossibly high Lorentz factor for the collapsar model, dynamic neutron decoupling will not occur.

There may be a detectable neutrino signature of dynamic neutron decoupling. Neutron-proton collisions occurring during decoupling will generate pions. In turn these pions will decay and lead to the generation of neutrinos with energies of a few GeV in our reference frame. These neutrinos should be detectable at the rate of about one per year in next generation neutrino telescopes (Bahcall & Mészáros 2000). In addition, there may also be a direct electromagnetic signature of neutron decoupling. For some bursts arising from external shocks, a slow decoupled neutron shell will decay and shock with the outer proton shell as the outer shell plows into the interstellar medium. This leads to a characteristic two-peaked structure in the burst (Pruet & Dalal 2002).

Regardless of whether dynamic neutron decoupling occurs, neutrons in the jet may have observable implications for the GRB afterglow. This is particularly true when the shocking radius, i.e. the radius at which the shocks giving rise to the observed  $\gamma$ -rays occur, is smaller than the length over which free neutrons decay. This condition is

$$r_{\text{shock}} \lesssim \gamma_2 \tau_n c \approx 10^{15} \gamma_2 \text{cm}, \quad (13)$$

where  $r_{\text{shock}}$  is the shocking radius,  $\gamma_2$  is the Lorentz factor of the outflow in units of 100, and  $\tau_n \sim 1000 \text{sec}$  is the free neutron lifetime. Eq. 13 is generally satisfied for bursts from internal shocks and bursts from external shocks in a very dense medium. When Eq. 13 holds, the neutrons can stream ahead of the slowing proton shell (the complement of the dynamic neutron decoupling discussed above) and deposit energy as they decay. Implications for the resulting afterglow in such a case have been discussed by Beloborodov (2002).

In the next section we discuss the  $r$ -process in winds and jets from accretion disks. However, we first note that GRB jets are characterized by interesting light element synthesis. Pruet, Guiles, & Fuller (2002) and Lemoine (2002) calculated the thermal synthesis of light elements in GRB-like outflows. They find that the final deuterium mass fraction can be of order 1%, some three orders of magnitude larger than the primordial yield. For kinematically well coupled flows, the nucleosynthesis depends sensitively on  $Y_e$ , with deuterium yield decreasing with increasing neutron excess. For flows in which dynamic neutron decoupling occurs, high energy neutron- $\alpha$  collisions will spall deuterons and can result in final deuteron mass fractions as high as 10% (Pruet, Guiles, & Fuller 2002).

### 4.3. The $r$ -process

There are two possible sites for the  $r$ -process here in those cases where  $Y_e$  is low - in the jet and in the disk wind.

#### 4.3.1. In the jet

The jet has the merit of originating in the vicinity of the black hole where the neutron excess is likely to be greatest. If magnetic fields drive the heating and initial acceleration of the jet, then this neutron excess will likely be preserved. If neutrinos drive the outflow (MacFadyen & Woosley 1999),  $Y_e$  will be reset to some extent by the weak interactions. However, if the details of the outflow above the black hole are similar to spherically symmetric neutrino driven ultra-relativistic winds, then only  $\nu\bar{\nu}$  annihilation will be important and the flow will remain neutron rich (Pruet, Fuller, & Cardall 2001).

It is clear that the rapid expansion of the jet will be favorable to freezing out with a large abundance of free neutrons and this is conducive to the  $r$ -process (Hoffman, Woosley, & Qian 1997). However, a pure nucleonic jet coming from the adiabatic expansion of a fireball with energy loading  $\eta = E_{\text{internal}}/\rho c^2 \gtrsim 100$  is too much of a good thing when it comes to entropy and rapid expansion. The entropy was given in eq. 12 (Qian & Woosley 1996)

$$s/k = \frac{11\pi^2}{45} \left(\frac{kT}{\hbar c}\right)^3 m_N / \rho \quad (14)$$

The internal energy (erg/gm) is

$$\epsilon = \frac{11\pi^2}{60} \left(\frac{kT}{\hbar c}\right)^4 1/\rho \quad (15)$$

and hence, for  $\eta = 200$  and  $kT \sim 2$  MeV

$$s/k_b = \frac{4}{3} \frac{\eta c^2 m_N}{kT} \sim 10^5. \quad (16)$$

The time scale for the expansion,  $r/c$ , is less than a millisecond. The high entropy implies a low density at the temperature when  $n$  and  $p$  can start to recombine. Coupled with the rapid expansion, one might conclude that the jet will remain pure nucleons and light nuclei and that an  $r$ -process is impossible.

This conclusion would be erroneous on several counts. First, the jet may not always have such high energy loading. There may be cases where no gamma-ray burst is produced and the energy loading of the jet is much less. The entropy would then decrease and the expansion time scale would increase. Whether to call these “dirty fireballs” or simply an extension of the “disk wind” is simply a matter of taste (see below).

Of more relevance to GRB models, and particularly to those that involve massive stars, is that the jet will not escape the star without interaction. Along the walls of the jet, the Kelvin Helmholtz instability will occur (Zhang & Woosley 2002). The jet will also encounter one or more shocks where it will be abruptly slowed. Most interesting is the “jet head” which

moves through the star subrelativistically with a speed that varies but is of order  $c/3$ . At this head the jet mixes with stellar material and the mixture is swept backwards (in the moving frame) forming a cocoon. It typically takes 5 to 10 sec for the jet head to penetrate the roughly one solar radius of overlying Wolf-Rayet star in the collapsar model.

During this time, neutrons in the jet are mixed with heavy nuclei - He, O, Si, Ne, Mg and the like - which can serve as seeds for an  $r$ -process. The overall dynamics is likely to be quite complex and its study would require a multi-dimensional relativistic simulation well beyond the scope of this paper. However, Zhang & Woosley (2002) find typical densities and time scales in the jet prior to break out are  $10^{-4}$  to  $10^{-1}$  g cm $^{-3}$  and seconds. This is enough that many, if not all of the neutrons in the jet would capture.

Still, the overall yield in gamma-ray bursts is too small to account for the solar  $r$ -process. Assume there is one GRB for each 100 supernovae. Each burst has  $10^{51}$  -  $10^{52}$  erg of relativistic ejecta (both jets) and a Lorentz factor that is at least 200 (Lithwick & Sari 2001). The jet will be some mixture of entrained stellar material and jet, but assume that the initial jet is half or more of the relativistic ejecta. This gives an equivalent yield of about  $10^{-7} M_{\odot}$  per supernova. Probably the  $r$ -process will be at most 10% of this (the rest may be  $\alpha$ -particles and entrained nuclei). This then is several orders of magnitude less than required to make the solar  $r$ -process. However, GRB jets might still be important sources of the  $r$ -process in metal-deficient stars or of select rare nuclei in the sun.

#### 4.3.2. *The $r$ -process in the disk wind*

A more significant  $r$ -process could come from the non-relativistic ejecta that comprise the disk wind, provided that the entropy is increased by magnetic processes to well above its value in the middle of the disk, as in for example, Daigne & Mochkovitch (2002). Assume that the accretion is 50% efficient, that is that half the material that enters the disk eventually enters the black hole and the other half is blown away (Narayan, Piran, & Kumar 2002). A typical collapsar powered GRB involves the accretion of from one to several solar masses, so  $\sim 1 M_{\odot}$  is ejected from the disk. Most of this will not be neutron-rich enough or expand fast enough to make the  $r$ -process, but consider the implications if only 1% of the mass that is lost comes from the inner disk at times when the accretion rate is over  $0.1 M_{\odot} \text{ sec}^{-1}$  and  $Y_e < 0.4$ .

So close to the hole, significant entropy will be added by any acceleration process that produces a strong outflow. A crude estimate is  $s/k_b \sim GMm_n/(rkT_{max}) \sim 400 r_6^{-1} (2 \text{ MeV}/T_{max})$  (Qian & Woosley 1996), where  $T_{max}$  is the temperature where the energy deposition is the

greatest. In fact the conditions in the inner disk for accretion rates  $\sim 0.1 M_{\odot} \text{ sec}^{-1}$  are not so different - in terms of neutrino luminosity, neutron excess, temperature, and gravitational potential - from the neutrino-driven wind in an ordinary supernova, and one might expect a similar  $r$ -process (Woosley et al. 1994). The gravitational potential though, can in principle, be greater and a larger entropy and shorter time scale might be realized. Assume that the ejecta will be very rich in  $\alpha$ -particles and contain of order 10%  $r$ -process by mass. Putting the numbers together then gives an  $r$ -process synthesis equivalent to  $10^{-5} M_{\odot}$  per supernova, making this possibility well worth further investigation.

The authors acknowledge helpful correspondence with Weiqun Zhang regarding the conditions in collapsar jets. This research has been supported by NASA (NAG5-8128, NAG5-12036, and MIT-292701) and the DOE Program for Scientific Discovery through Advanced Computing (SciDAC; DE-FC02-01ER41176). A portion of this work was performed under the auspices of the U.S. Department of Energy by University of California Lawrence Livermore Laboratory under contract W-7405-ENG-48.

## REFERENCES

- Bahcall, J. N. & Mészáros, P. 2000, Phys. Rev. Lett. 85, 1362.
- Beloborodov, A. M. 2002, astro-ph/0209228.
- Bloom, J. S., Kulkarni, S. R., Price, P. A., Reichart, D., Galama, T. J., Schmidt, B. P., Frail, D. A., Berger, E., et al 2002, ApJ, 572, L45
- Daigne, F., & Mochkovitch, R. 2002 A&A, 388, 189
- Derishev, E. V., Kocharovsky, V. V., & Kocharovsky, V. V. 1999, A&A, 345, 51.
- Di Matteo, T., Perna, R., & Narayan, R. 2002 A&A, 390, L35 (astro-ph 0207319)
- Eichler, D., Livio, M., Piran, T., & Schramm, D. N. 1989, Nature, 340, 126
- Frail, D., et al. 2001, ApJ, 562, L55
- Freedman, D. L., & Waxman, E. 2001, ApJ, 547, 922
- Fryer, C. L., Woosley, S. E., Herant, M., & Davies, M. B. 1999 ApJ, 520, 650
- Fryer, C. L., Woosley, S. E., & Hartmann, D. H. 1999, ApJ, 526, 152

- Fuller, G. M., Fowler, W. A., & Newman, M. J. 1982, *ApJ*, 252, 715.
- Fuller, G. M., Pruet, J., & Abazajian, K. 2000, *Phys. Rev. Lett.*, 85, 2673.
- Galama, T. J., Vreeswijk, P. M., van Paradijs, J., Kouveliotou, C., Augusteijn, T., Bohnhardt, H., Brewer, J. P., Doublier, V., et al. 1998, *Nature*, 395, 670
- Hartmann, D., Woosley, S. E., & El Eid, M. 1985 *ApJ*, 297, 837 97ApJ...482..951H
- Hoffman, R. D., Woosley, S. E., & Qian, Y.-Z. 1997, *ApJ*, 482, 951
- Janka, H.-T., Eberl, T., Ruffert, M., & Fryer, C. L. 1999 *ApJ*, 527, 39
- Lemoine, M. 2002, *A&A* letters, in press.
- Lithwick, Y., & Sari, R. 2001, *ApJ*, 555, 540
- MacFadyen, A. I., & Woosley, S. E. 1999, *ApJ*, 524, 262
- MacFadyen, A. I., Woosley, S. E., & Heger, A. 2001, *ApJ*, 550, 410
- Narayan, R., Piran, T., Kumar, P. 2001 *ApJ*, 557, 949
- Popham, R., Woosley, S. E., & Fryer C. L 1999, *ApJ*, 518, 356
- Pruet, J., & Dalal, N. 2002, *ApJ*, 573, 770
- Pruet, J., Fuller, G. M., & Cardall, C.Y. 2001, *ApJ*, 561, 957
- Pruet, J., Guiles, S., & Fuller 2002, *ApJ*, in press.
- Qian, Y.-Z., & Woosley, S. E. 1996, *ApJ*, 471, 331
- Ruffert, M., & Janka, H.-Th. 2001, *A&A*, 380, 544
- Vietri, M., & Stella, L. 1998, *ApJ*, 507, L45
- Vietri, M., & Stella, L. 1999, *ApJ*, 527, L43
- Woosley, S. E., Arnett, W. D., & Clayton, D. D. 1973, *ApJS*, 26, 231
- Woosley, S. E. 1993, *ApJ*, 405, 273
- Woosley, S. E., Wilson, J. R., Mathews, G. J., Hoffman, R. D., & Meyer, B. S. 1994, *ApJ*, 433, 229
- Zhang, W., & Fryer, C. L 2001 *ApJ*, 550, 357

Zhang, W. & Woosley, S. E. 2002, ApJ, submitted, astro-ph/0207436

Table 1. Electron Mole Number Near the Event Horizon

Model	$\dot{M}^a$	$\alpha^b$	$Y_e$
A	0.01	0.1	0.510
B	0.1	0.1	0.435
C	0.1	0.03	0.119
D	0.1	0.01	0.045
E	1.0	0.1	0.115
F <sup>c</sup>	0.03	0.1	0.527
G <sup>d</sup>	0.1	0.1	0.077

<sup>a</sup>Accretion rate in  $M_\odot \text{ sec}^{-1}$

<sup>b</sup>Disk viscosity

<sup>c</sup>Disk properties inferred from the scaling relations in Popham, Woosley, & Fryer (1999) for this model.

<sup>d</sup>Kerr parameter  $a = 0.95$  for this model.



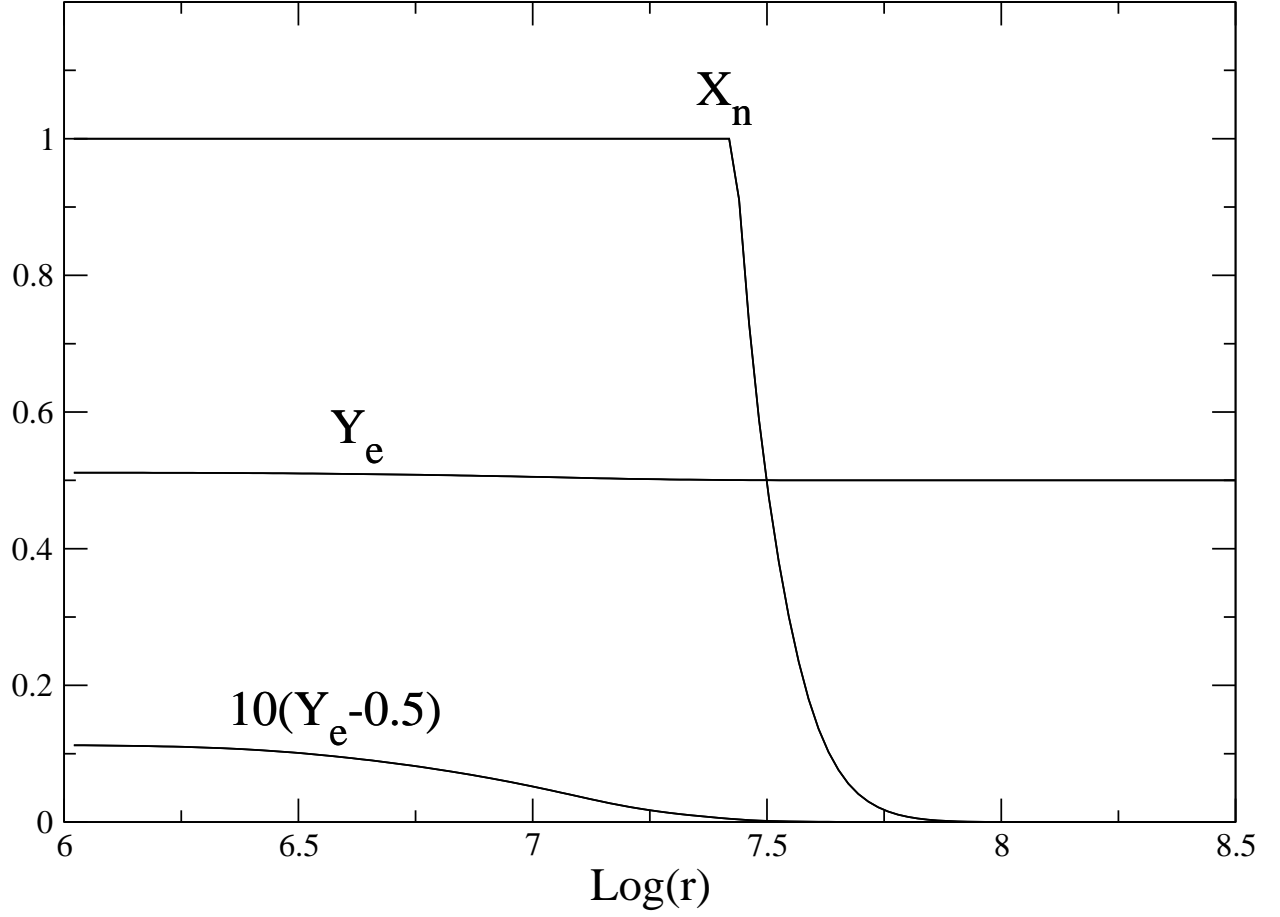


Fig. 1.— Evolution of  $Y_e$  and the free nucleon mass fraction  $X_n$  in a disk with  $\dot{M} = 0.01M_\odot \text{ sec}^{-1}$  and  $\alpha = 0.1$ .

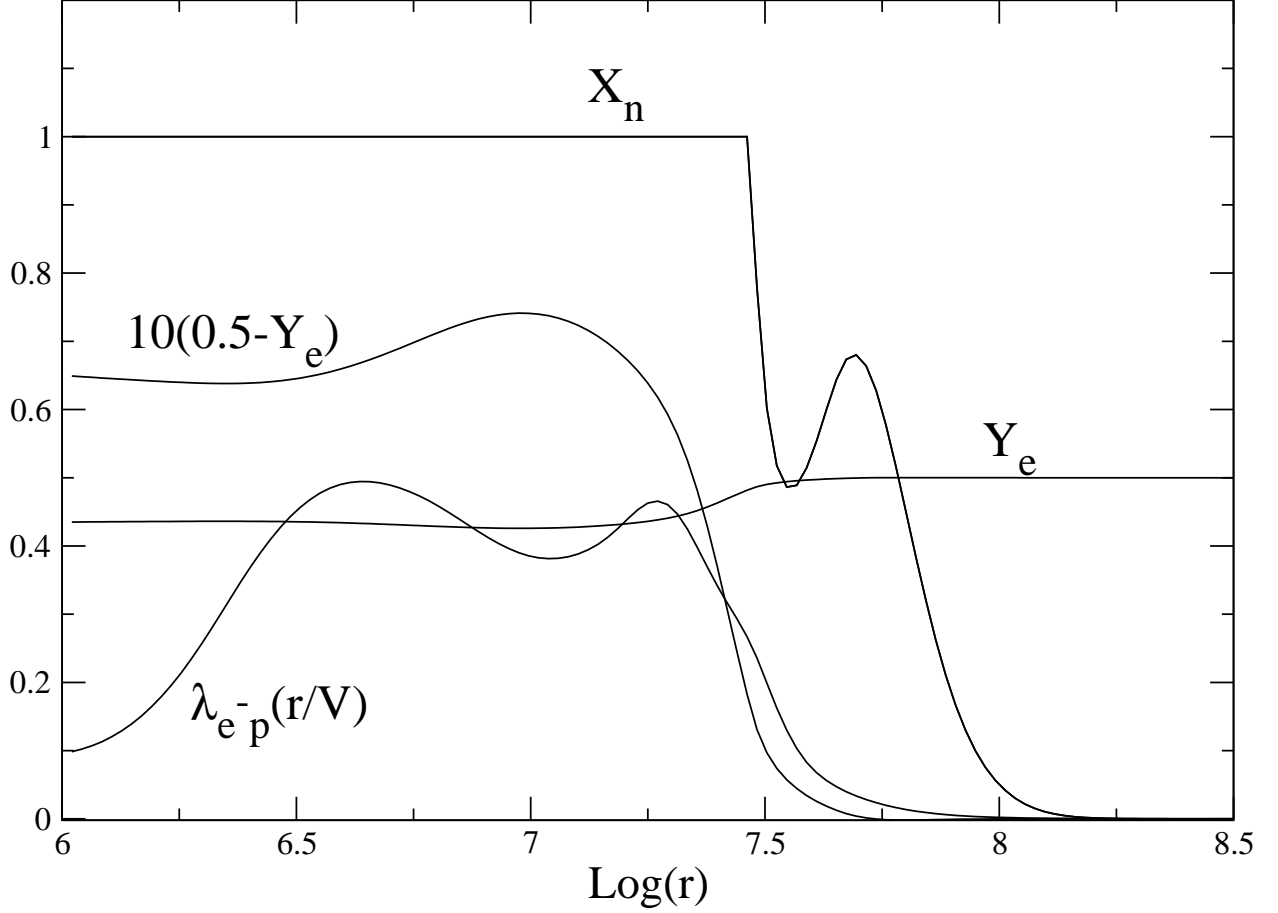


Fig. 2.— Evolution of  $Y_e$  and  $X_n$  in a disk with  $\dot{M} = 0.1 M_\odot \text{ sec}^{-1}$  and  $\alpha = 0.1$ . Shown also is the quantity  $\lambda_{e-p}(r/V)$ , a rough measure of whether or not there is time for  $Y_e$  to come to equilibrium with respect to  $e^\pm$  capture.

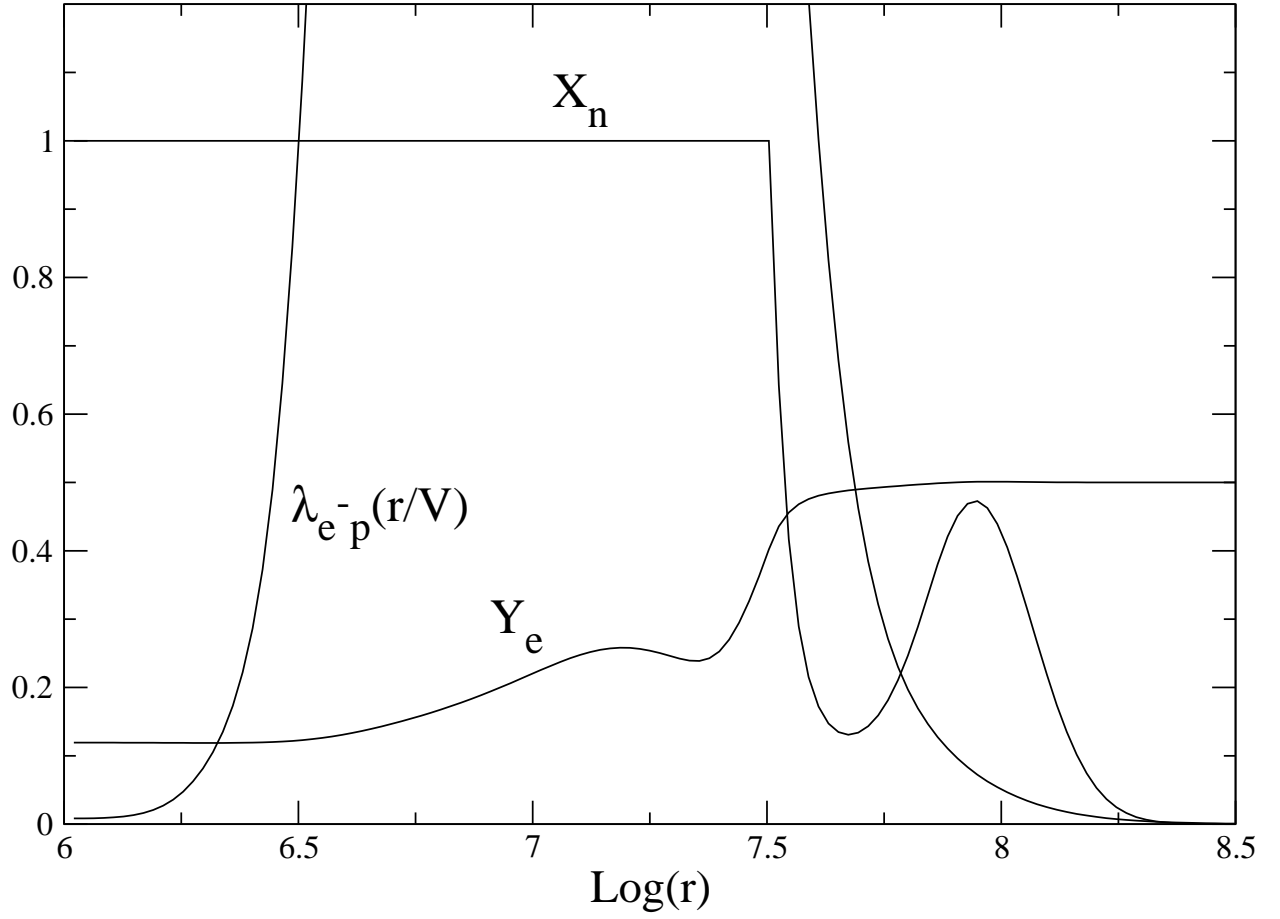


Fig. 3.— Same as Fig. 2, except for  $\dot{M} = 0.1 M_\odot \text{ sec}^{-1}$  and  $\alpha = 0.03$ .

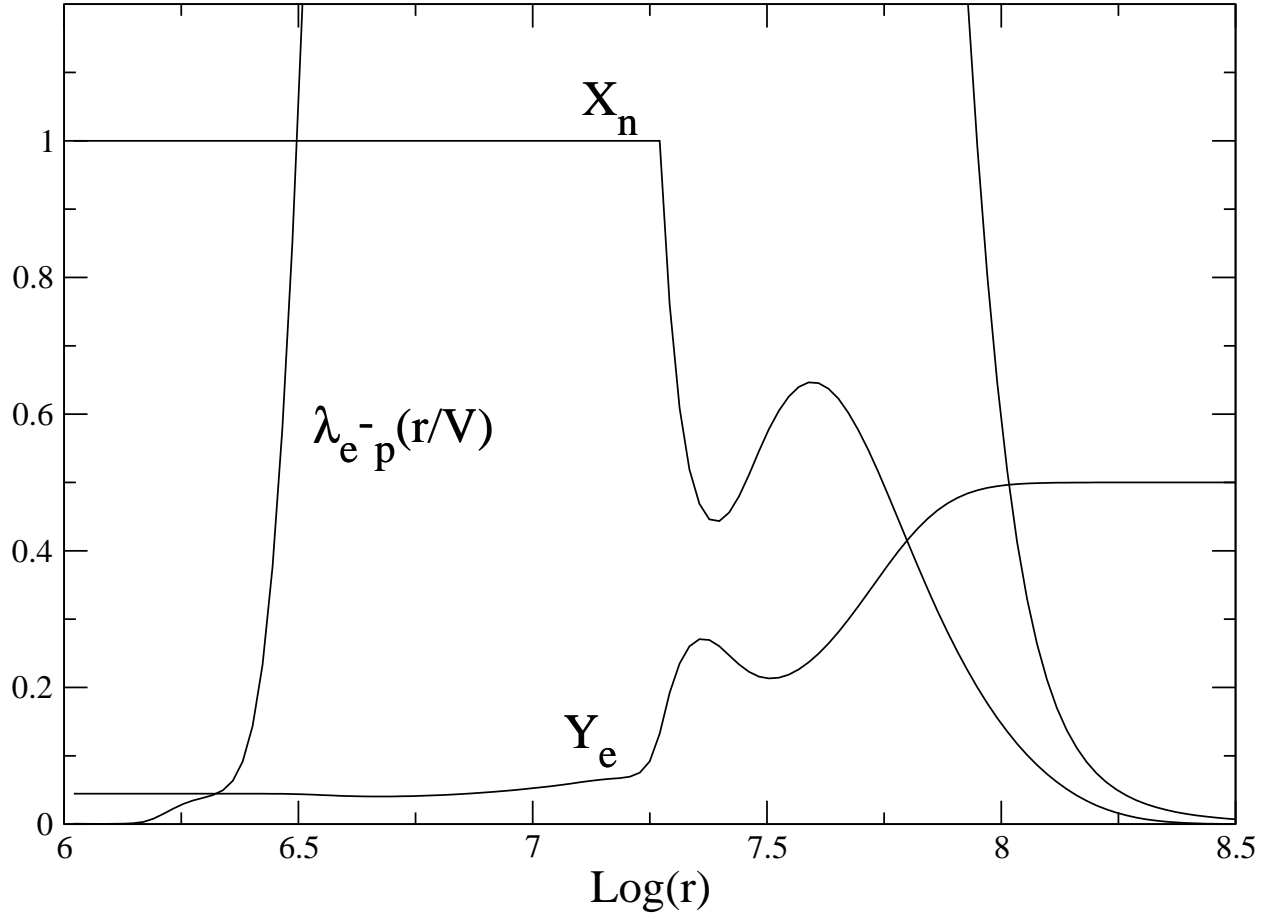


Fig. 4.— Same as Fig. 2, except for  $\dot{M} = 0.1 M_\odot \text{ sec}^{-1}$  and  $\alpha = 0.01$ .

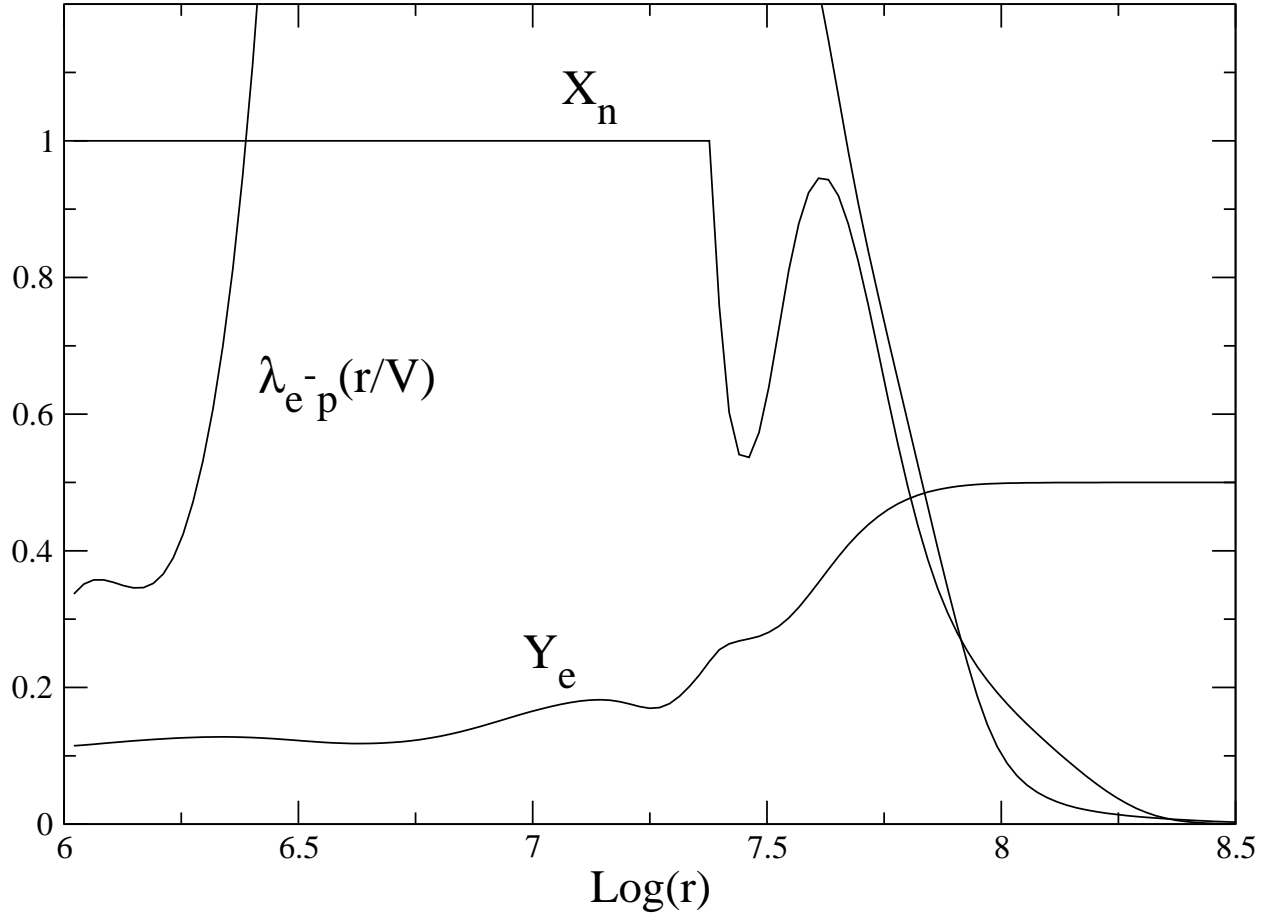


Fig. 5.— Same as Fig. 2, except for  $\dot{M} = 1M_{\odot} \text{ sec}^{-1}$  and  $\alpha = 0.1$ .

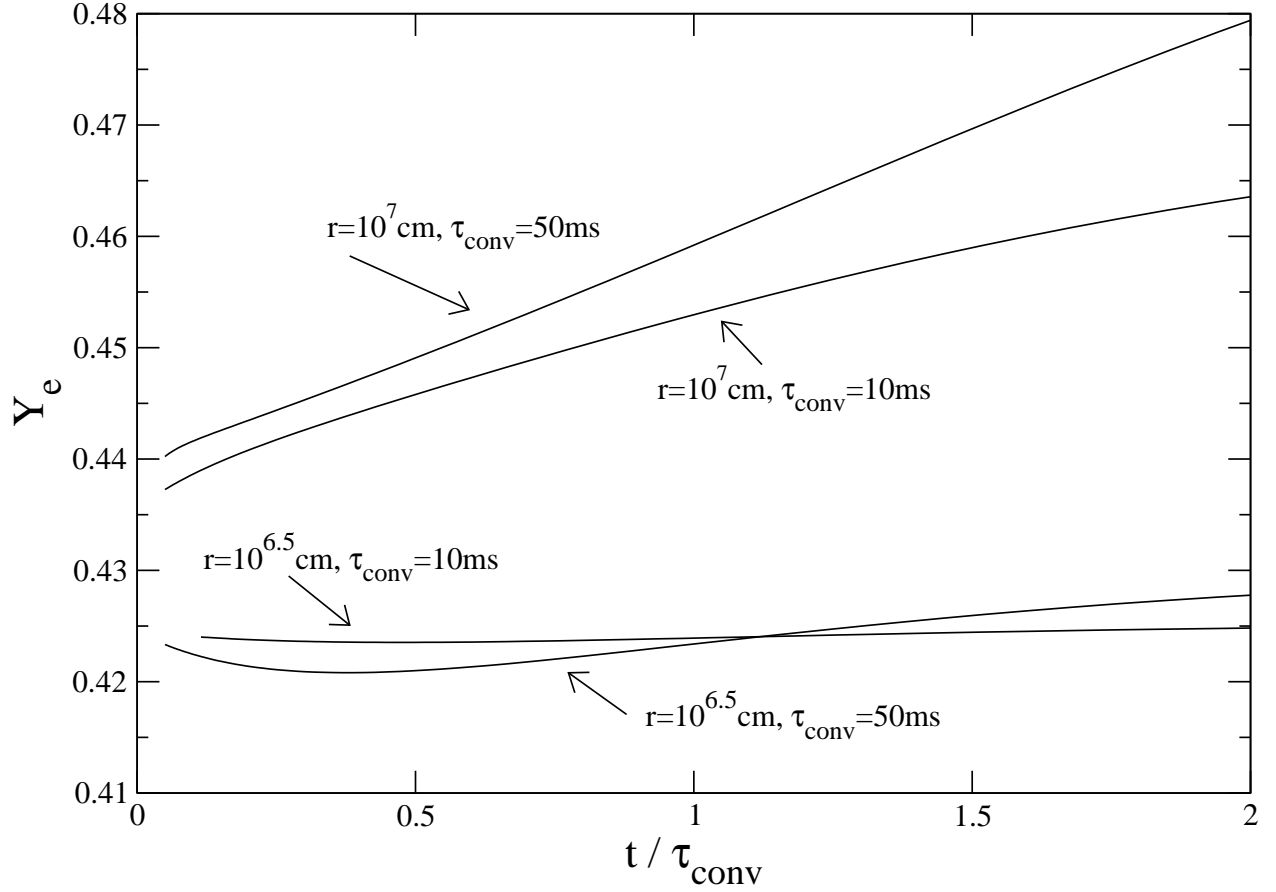


Fig. 6.— Evolution of electron fraction in a convective and adiabatic fluid element in a disk with  $\dot{M} = 0.1 M_{\odot} \text{ sec}^{-1}$  and  $\alpha = 0.1$ . The assumed convective timescale  $\tau_{\text{conv}}$  and radius in the disk from which the material originates is given next to each curve.

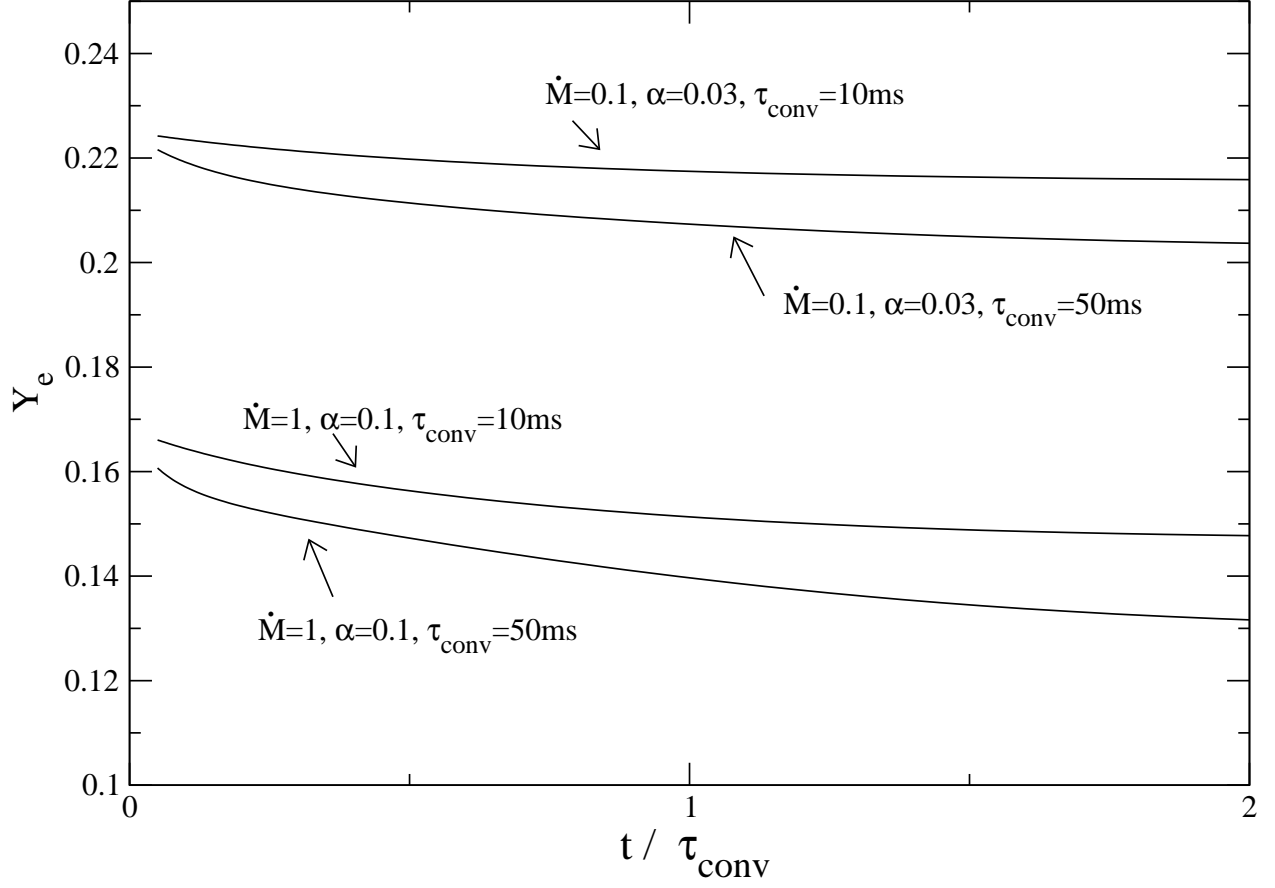


Fig. 7.— Evolution of electron fraction in a convective and adiabatic fluid element in two different disks characterized by low electron fractions. The assumed convective timescale and disk parameters are given next to each curve. In all cases the material is assumed to originate from  $r = 10^7\text{cm}$ .